

This is the peer reviewed version of the following article: Phe, R.Z.H. and Skelton, B.W. and Massi, M. and Ogden, M.I. 2020. Influence of the para-Substituent in Lanthanoid Complexes of Bis-Tetrazole-Substituted Calix[4]arenes. European Journal of Inorganic Chemistry. 2020 (1): pp. 94-100, which has been published in final form at 10.1002/ejic.201900877. This article may be used for non-commercial purposes in accordance with Wiley Terms and Conditions for Use of Self-Archived Versions.

## Table of Contents

Ligand Synthesis .....	2
25,27-Dihydroxy-26,28-bis(tetrazole-5-ylmethoxy)calix[4]arene <b>2</b> .....	2
5,11,17,23-Tetra-allyl-25,27-dihydroxy-26,28-dicyanomethoxycalix[4]arene <b>4</b> .....	4
General synthesis for Ln(NO <sub>3</sub> ) <sub>3</sub> (DMSO) <sub>4</sub> salts .....	5
Dynamic Light Scattering .....	6
Microanalysis of the metal complexes .....	7
Complexes of <b>2</b> crystallised from ethanol .....	7
Complexes of <b>2</b> crystallised from acetonitrile .....	7
Complexes of <b>3</b> crystallised from ethanol/ethyl acetate .....	8
Crystal Structure Supplementary Information .....	8
Solution phase photophysical studies of Ln complexes of calixarene <b>2</b> .....	14
References .....	16

## Ligand Synthesis

### 25,27-Dihydroxy-26,28-bis(tetrazole-5-ylmethoxy)calix[4]arene **2**

Triethylamine (583  $\mu\text{L}$ , 4.18 mmol) and 33 % hydrochloric acid (302  $\mu\text{L}$ , 2.99  $\mu\text{mol}$ ) were added to cold toluene (150 mL) over an ice bath and the reaction flask was stoppered immediately. The colourless mixture was stirred for 10 min to allow the evolved white gas to dissolve into solution. 25,27-Dihydroxy-26,28-dicyanomethoxycalix[4]arene<sup>[1]</sup> (500 mg, 995  $\mu\text{mol}$ ) and sodium azide (246 mg, 3.78 mmol) were added to the colourless solution and the reaction mixture was heated at 70  $^{\circ}\text{C}$  for 24 hr. The cloudy white reaction mixture was cooled to room temperature. The white precipitate was collected via vacuum filtration, dissolved in ethyl acetate (60 mL) and then washed with 1M hydrochloric acid (3x 15 mL). The organic fraction was dried over magnesium sulphate (*ca.* 0.3 g) and filtered. The solvent from the clear colourless mixture was removed via rotary evaporator to afford a white residue. Ethanol (20 mL) was added to the crude product and sonicated in the water bath for 5 min. The resulting white solid (498 mg, 85 %) was collected via vacuum filtration. Analytical pure samples can be attained by recrystallisation of the white solid using ethanol to afford a white semi-crystalline product. M.P. 230-231  $^{\circ}\text{C}$  (dec.) [lit. 239-240  $^{\circ}\text{C}$ ]<sup>[2]</sup>.

IR (ATR)  $\nu$   $\text{cm}^{-1}$  3356 (b, OH), 3037 (w, aromatic CH), 2928 (w, aliphatic CH), 2878 (w, aliphatic CH), 1590 (w, aromatic C=C), 1558 (w, aromatic C=C), 1464 (s, aromatic C=C) and 1436 (m, aromatic C=C).

$^1\text{H}$  NMR ( $\text{CD}_3\text{CN}$ )  $\delta$  ppm 7.16 (d, 4H, Ar-H,  $J=7.6$  Hz), 7.04 (d, 4H, Ar-H,  $J=7.6$  Hz), 6.88 (t, 2H, Ar-H,  $J=7.6$  Hz), 6.72 (t, 2H, Ar-H,  $J=7.6$  Hz), 5.46 (s, 4H, Ar-O-CH<sub>2</sub>), 4.18 (d, 4H, axial Ar-CH<sub>2</sub>-Ar,  $J=13.6$  Hz) and 3.47 (d, 4H, equatorial Ar-CH<sub>2</sub>-Ar,  $J=13.6$  Hz).

$^{13}\text{C}$  NMR ( $\text{CD}_3\text{CN}$ )  $\delta$  ppm 153.05 (Ar-C-O), 152.32 (Ar-C-OH), 134.77 (Ar-C), 130.35 (Ar-CH), 129.93 (Ar-CH), 128.80 (Ar-C), 127.33 (Ar-CH), 121.29 (Ar-CH), 68.11 (O-CH<sub>2</sub>-N) and 31.67 (Ar-CH<sub>2</sub>-Ar).

Anal. Calculated for  $\text{C}_{32}\text{H}_{28}\text{N}_8\text{O}_4 \cdot 1[\text{C}_2\text{H}_6\text{O}]$ : C, 64.34; H, 5.40; N, 17.65%. Found C, 64.24; H, 5.42; N, 17.57%.

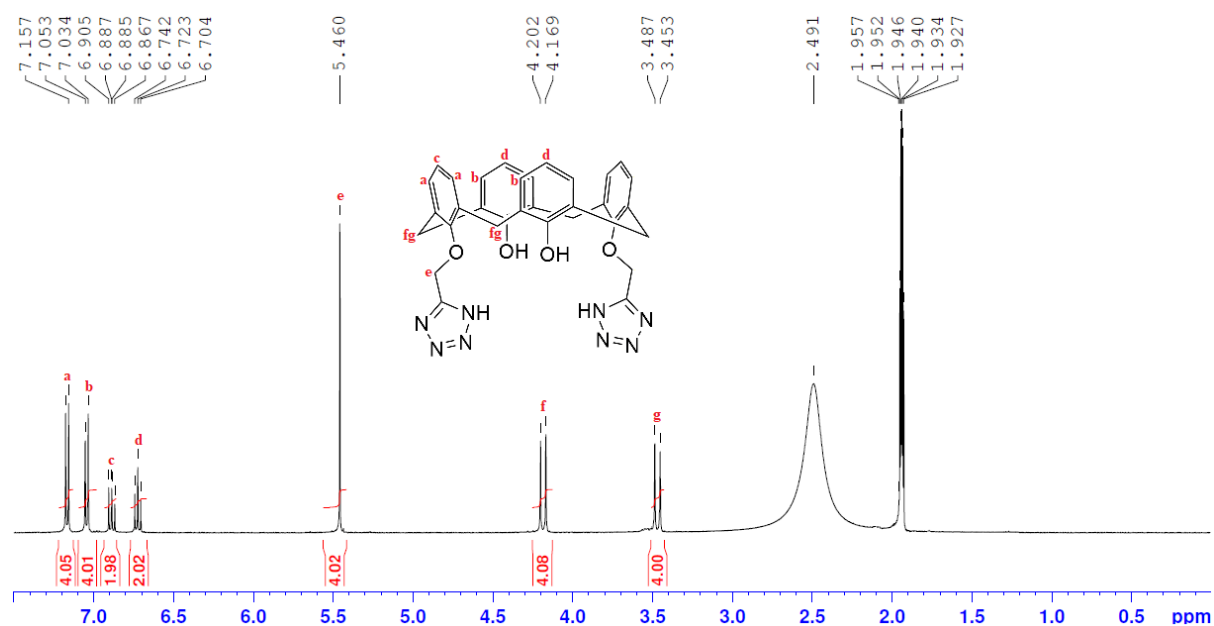


Figure S1:  $^1\text{H}$  NMR spectrum of **2**

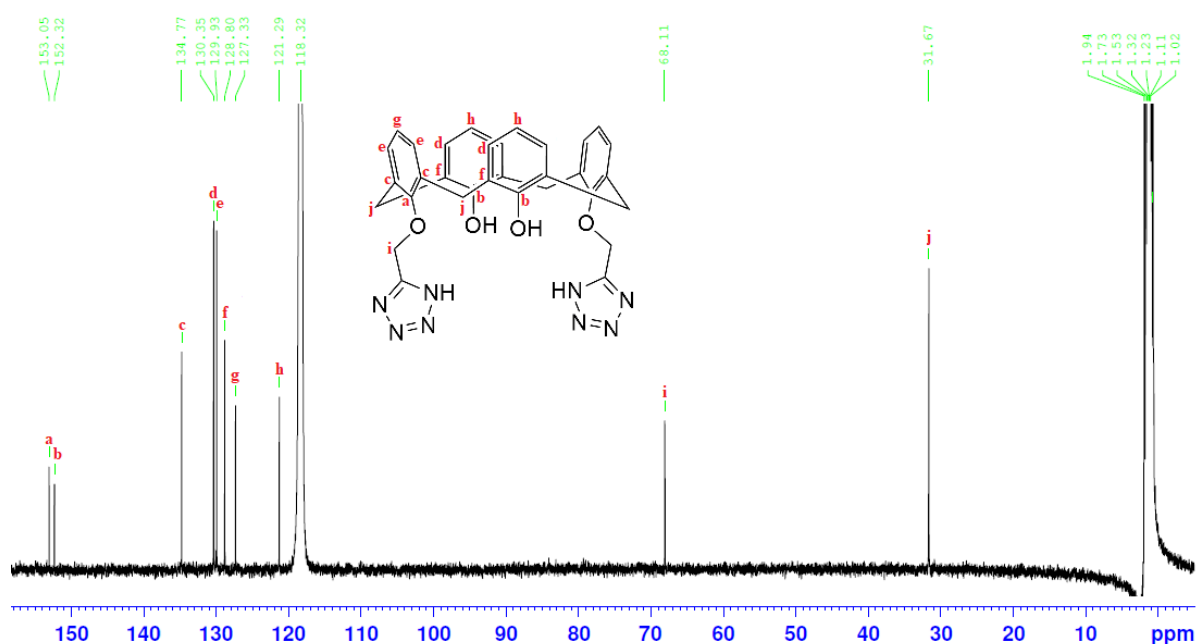


Figure S2: :  $^{13}\text{C}$  NMR spectrum of **2**

*5,11,17,23-Tetra-allyl-25,27-dihydroxy-26,28-bis(tetrazole-5-ylmethoxy)calix[4]arene 3*

Triethylamine (884  $\mu\text{L}$ , 6.34 mmol) and 33 % hydrochloric acid (456  $\mu\text{L}$ , 4.53  $\mu\text{mol}$ ) were added to cold toluene (100 mL) over an ice bath and the reaction flask was stoppered immediately. The colourless mixture was stirred for 10 min to allow the evolved white gas to dissolve into solution. 5,11,17,23-Tetra-allyl-25,27-dihydroxy-26,28-dicyanomethoxycalix[4]arene **4** (1.00 g, 1.51 mmol) and sodium azide (373 mg, 5.73 mmol) were added to the colourless solution and the reaction mixture was heated at 70  $^{\circ}\text{C}$  for 72 hr. The yellow reaction mixture was cooled to room temperature. The solvent from the yellow mixture was removed via rotary evaporator. The resulting orange residue was dissolved in ethyl acetate (60 mL) and washed with 1M hydrochloric acid (3x 15 mL). The organic fraction was dried over magnesium sulphate (*ca.* 0.3 g) and filtered. The solvent was then concentrated in rotary evaporator to about 5 mL and diethyl ether (*ca.* 25 mL) was added. The orange precipitate impurities were removed via vacuum filtration and petroleum spirits (*ca.* 50 mL) was added to the clear colourless filtrate. The resulting white precipitate was collected via vacuum filtration to afford an off white solid (950 mg, 84 %). M.P. 150  $^{\circ}\text{C}$  (dec.). NMR data (Figure S3, Figure S4) indicated that the product was at most 95% pure, and this material was used for metal complexation studies as it was unable to be further purified. Single crystal x-ray structure determination of the metal complexes confirmed that the structure of calixarene **3** was correctly assigned.

IR (ATR)  $\nu$   $\text{cm}^{-1}$  3076-3005 (w, aromatic CH), 2977-2922 (w, aliphatic CH), 1638 (w, aromatic C=C) and 1473 (s, aromatic C=C).

$^1\text{H}$  NMR ( $\text{CDCl}_3$ )  $\delta$  ppm 6.89 (s, 4H, Ar-H), 6.86 (s, 4H, Ar-H), 5.84 (m, 4H,  $\text{CH}_2\text{-CH=CH}_2$ ), 5.46 (s, 4H, Ar-O- $\text{CH}_2$ ), 5.02 (m, 8H,  $\text{CH=CH}_2$ ), 4.10 (d, 4H, axial Ar- $\text{CH}_2$ -Ar), 3.48 (d, 4H, equatorial Ar- $\text{CH}_2$ -Ar), 3.24 (d, 4H, Ar- $\text{CH}_2$ -CH) and 3.17 (d, 4H, Ar- $\text{CH}_2$ -CH).

$^{13}\text{C}$  NMR ( $\text{CDCl}_3$ )  $\delta$  ppm 150.03 (Ar-C-O), 149.65 (Ar-C-OH), 138.53 (Ar-C), 137.83 ( $\text{CH}_2\text{-CH=CH}_2$ ), 137.02 (Ar-C), 136.94 ( $\text{CH}_2\text{-CH=CH}_2$ ), 133.07 (Ar-C), 129.92 (Ar-CH), 129.29 (Ar-CH), 127.61 (Ar-C), 116.30 ( $\text{CH=CH}_2$ ), 115.71 ( $\text{CH=CH}_2$ ), 68.71 (O- $\text{CH}_2$ -C), 39.70 (Ar- $\text{CH}_2$ -CH), 39.35 (Ar- $\text{CH}_2$ -CH) and 32.04 (Ar- $\text{CH}_2$ -Ar).

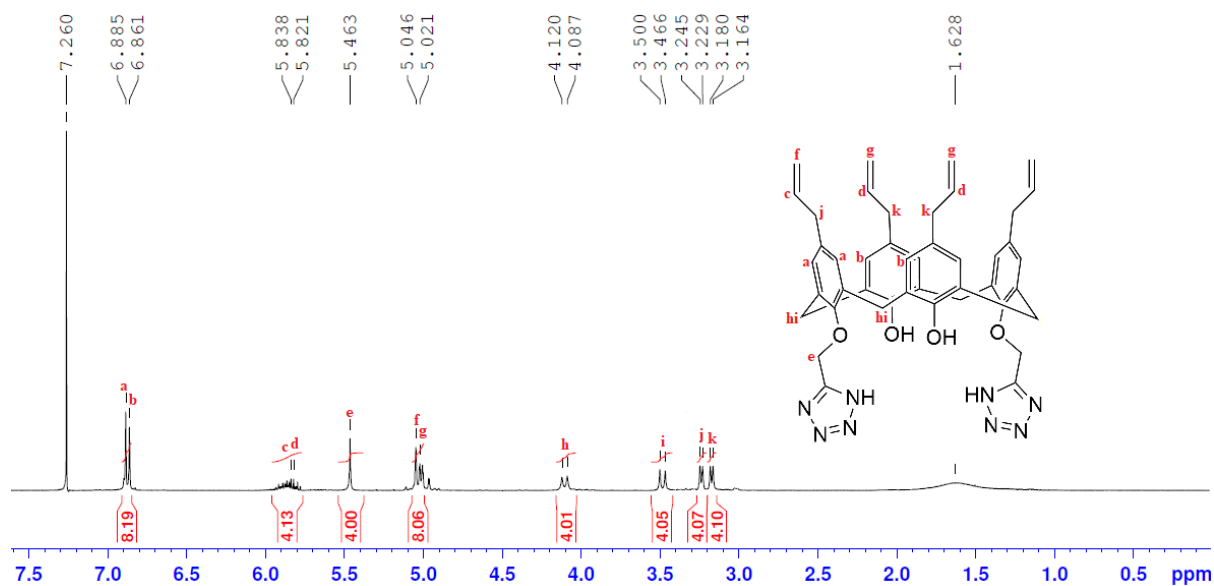


Figure S3:  $^1\text{H}$  NMR spectrum of **3**

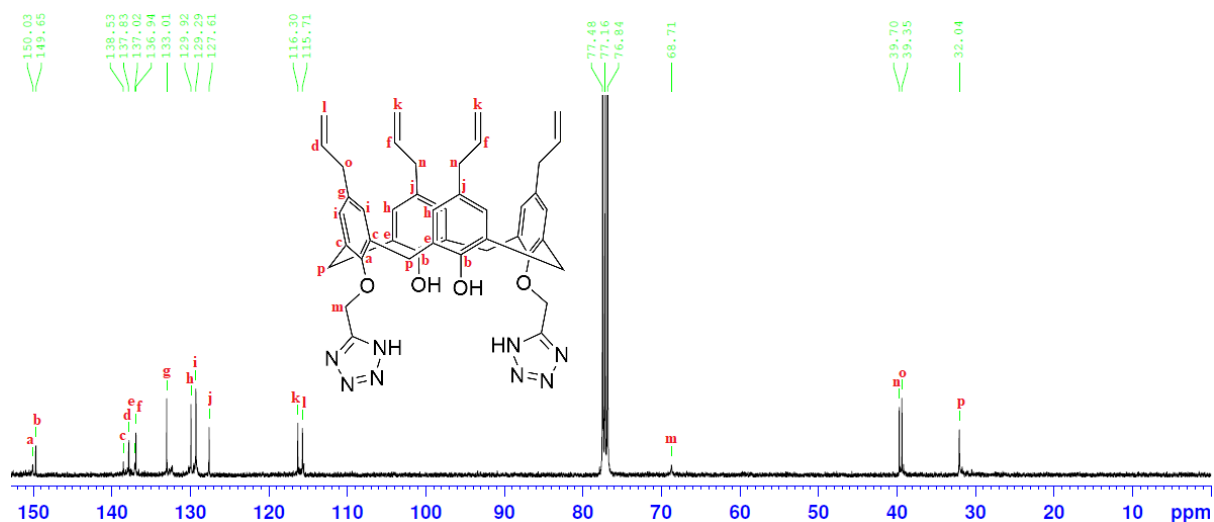


Figure S4:  $^{13}\text{C}$  NMR spectrum of **3**

#### 5,11,17,23-Tetra-allyl-25,27-dihydroxy-26,28-dicyanomethoxycalix[4]arene **4**

*p*-Allyl-calixarene<sup>[3]</sup> (2.000 g, 3.42 mmol) and potassium carbonate (1.654 g, 12.0 mmol) in dry acetone (120 mL) were stirred at room temperature under nitrogen atmosphere for 15 min. Bromoacetonitrile (1.406 mL, 20.2 mmol) was added to the opaque mixture and refluxed at 65 °C for 24 hr. The resulting yellow mixture was cooled to room temperature before being filtered and washed with dichloromethane (3x 30 mL). The solvent from the yellow filtrate was removed via rotary evaporator. Diethyl ether (15 mL) was added to the resulting brown oil, sonicated in a water bath and filtered. Petroleum spirits (40 mL) was added to the yellow filtrate and the resulting white precipitate was collected via vacuum filtration. The sticky pale white residue was re-dissolved in diethyl ether (15 mL), which was subsequently removed via rotary evaporator to afford a crude white solid (1.735 g, 77 %), that was not further purified.

$^1\text{H}$  NMR ( $\text{CDCl}_3$ )  $\delta$  ppm 6.92 (s, 4H, Ar-H), 6.64 (s, 4H, Ar-H), 5.99 (m, 2H,  $\text{CH}_2\text{-CH}=\text{CH}_2$ ), 5.91 (s, 2H, Ar-OH), 5.68 (m, 2H,  $\text{CH}_2\text{-CH}=\text{CH}_2$ ), 5.07 (m, 4H,  $\text{CH}=\text{CH}_2$ ), 4.87 (m, 4H,  $\text{CH}=\text{CH}_2$ ), 4.81 (s, 4H, Ar-O- $\text{CH}_2$ ),

4.21 (d, 4H, axial Ar-CH<sub>2</sub>-Ar), 3.45 (d, 4H, equatorial Ar-CH<sub>2</sub>-Ar), 3.31 (d, 2H, Ar-CH<sub>2</sub>-CH) and 3.03 (d, 2H, Ar-CH<sub>2</sub>-CH).

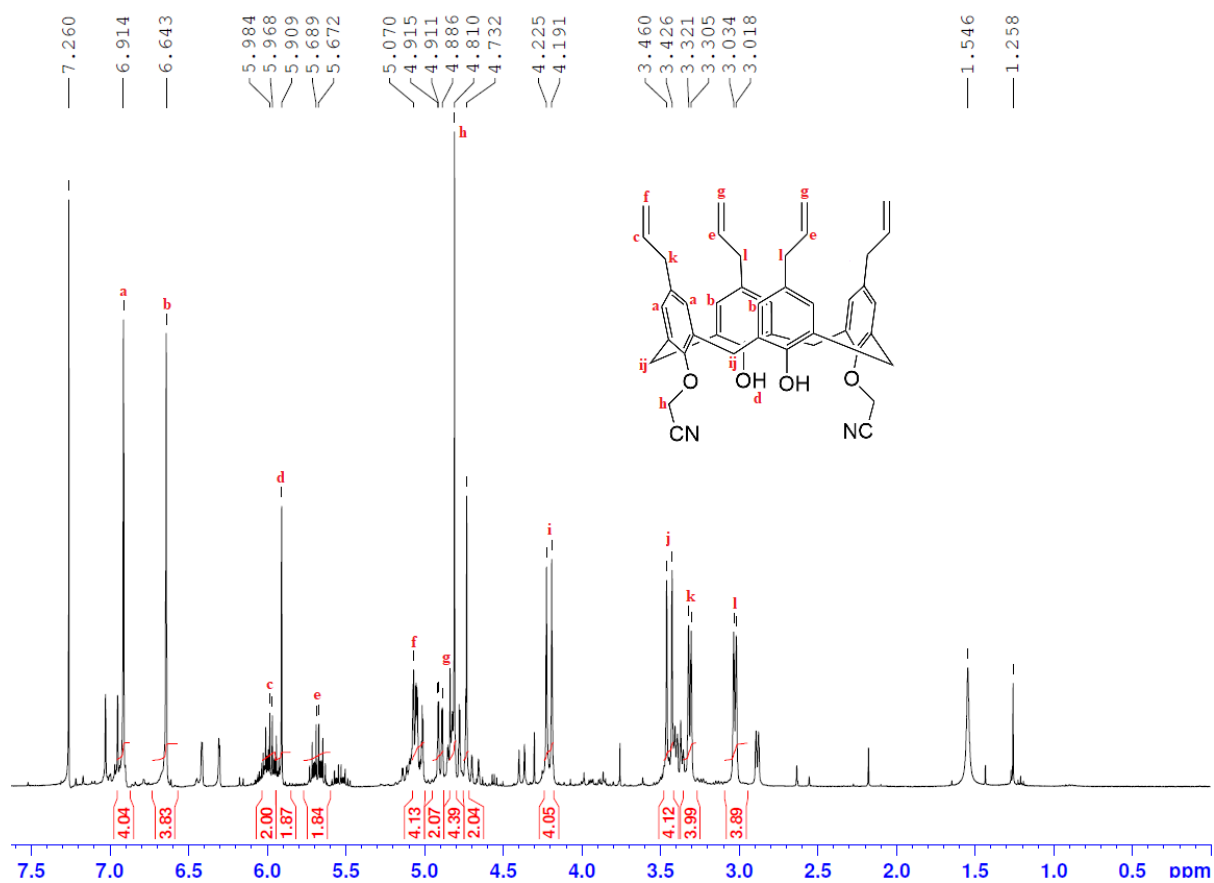


Figure S5. : <sup>1</sup>H NMR spectrum of 4

#### General synthesis for Ln(NO<sub>3</sub>)<sub>3</sub>(DMSO)<sub>3</sub> salts<sup>[4]</sup>

Ln<sub>2</sub>O<sub>3</sub> (1 eq.) was dissolved in concentrated nitric acid (5 mL) with gentle heating. Water (5 mL), dimethyl sulfoxide (8 eq.) and ethanol (25 mL) was sequentially added to the clear colourless solution while mixing. Diethyl ether (250 mL) was slowly added to the mixture and the clear mixture was allowed to stand for 15 min. The resulting precipitate was quickly collected via vacuum filtration and washed with diethyl ether (3x 5 mL) before storing the resulting crystals in a vacuum desiccator.

## Dynamic Light Scattering

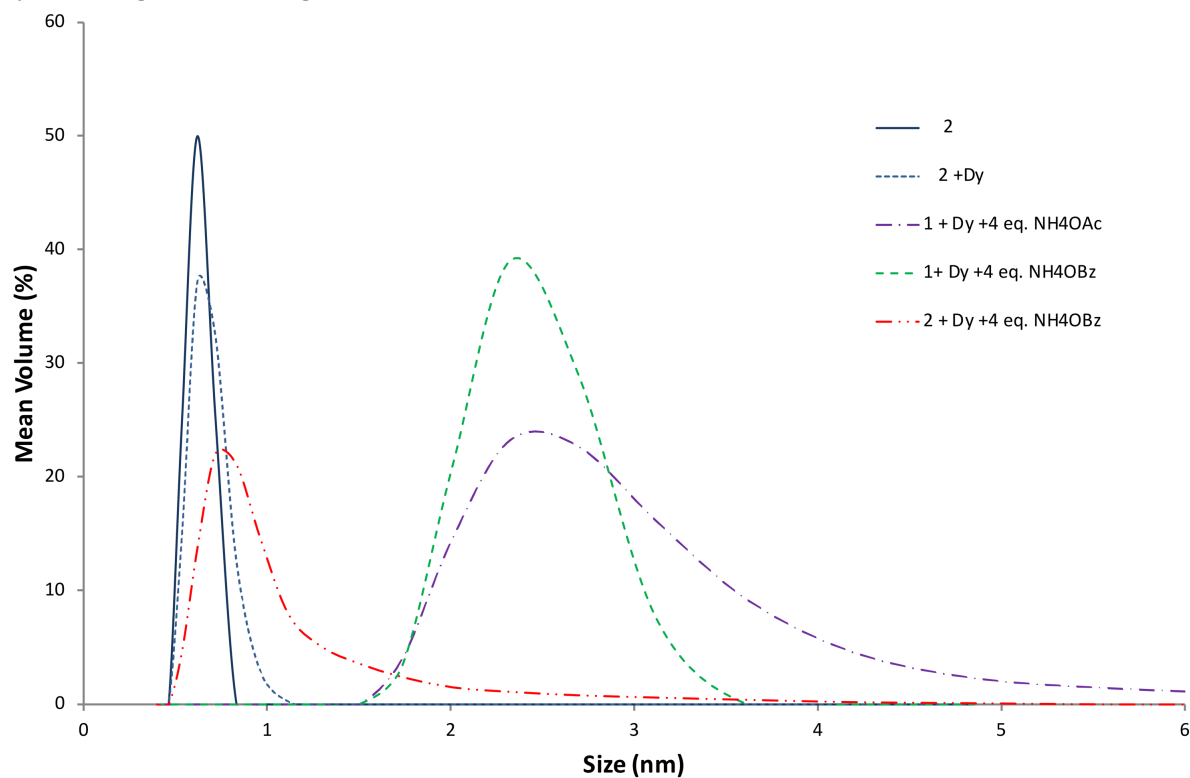


Figure S6. DLS results comparing the changes induced upon addition of aqueous ammonium carboxylates to solutions of *t*-butyl calixarene **2**, and the debutylated derivative **2**, in the presence of Dy.

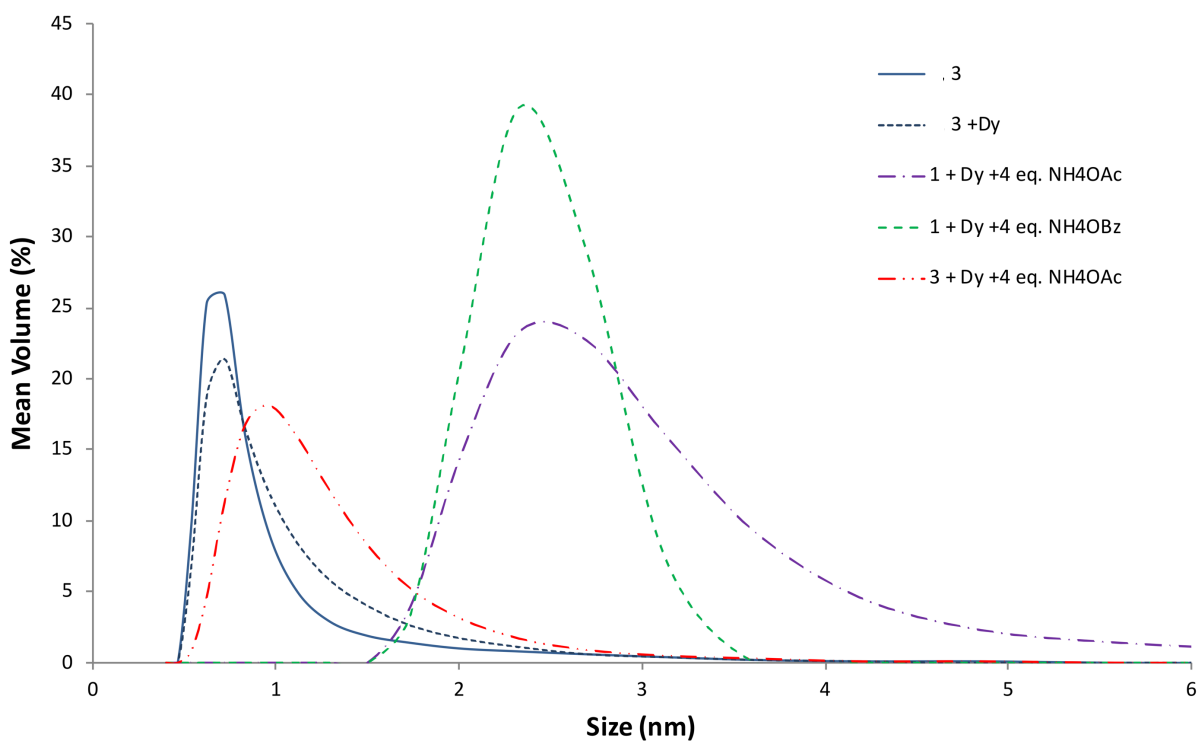


Figure S7. DLS results comparing the changes induced upon addition of aqueous ammonium carboxylates to solutions of *p*-*t*-butyl calixarene **3**, and the *p*-allyl derivative **3**, in the presence of Dy.

## Microanalysis of the metal complexes

Microanalysis of the metal complexes gave variable results, plausibly consistent with the variable solvation found through crystallography. In some cases the microanalysis matched the crystallographic results (rounding partial solvation modelled in the crystallography to the nearest whole number), and these are indicated below. In other cases, reasonable matches could be obtained only through assuming that some change in solvation occurred upon isolation of the metal complexes. Despite the variable results, microanalysis was useful in indicating that ammonium cations may be incorporated in the product, where initial modelling of the crystallographic structure was ambiguous. We note that fitting microanalytical data to the ethanol solvates required removing all or most of the ethanol molecules and replacing with water. We can not distinguish between this occurring upon isolation of the complex, or this being due to variable solvates formed in the original precipitate.

### *Complexes of 2 crystallised from ethanol*

Formula derived from crystallography:  $(\text{NH}_4)\text{Eu}(\mathbf{2-4H})(\text{EtOH})_4$ .

Calculated for  $\text{C}_{40}\text{H}_{52}\text{EuN}_9\text{O}_8$ : C, 51.2; H, 5.58; N, 13.4 %:

Found: C, 46.4; H, 4.57, N 14.6 %

Revised formula:  $(\text{NH}_4)\text{Eu}(\mathbf{2-4H})(\text{EtOH})(\text{H}_2\text{O})_4$

Calculated for  $\text{C}_{34}\text{H}_{42}\text{EuN}_9\text{O}_9$ : C, 46.8; H, 4.85; N, 14.4 %:

### *Complexes of 2 crystallised from acetonitrile*

Formula derived from crystallography:  $(\text{NH}_4)\text{Eu}(\mathbf{2-4H})(\text{H}_2\text{O})_3(\text{CH}_3\text{CN})$

Calculated for  $\text{C}_{34}\text{H}_{37}\text{EuN}_{10}\text{O}_7$ : C, 48.1; H, 4.39; N, 16.5 %:

Found: C, 46.2; H, 4.45, N 15.2 %

Revised formula:  $(\text{NH}_4)\text{Eu}(\mathbf{2-4H})(\text{H}_2\text{O})_4$

Calculated for  $\text{C}_{32}\text{H}_{36}\text{EuN}_9\text{O}_8$ : C, 46.5; H, 4.39; N, 15.2 %:

$(\text{NH}_4)\text{Tb}(\mathbf{2-4H})(\text{H}_2\text{O})_4$  – no crystal structure obtained, formula based on microanalysis

Found: , 46.3; H, 4.27, N 15.3 %

Calculated for  $\text{C}_{32}\text{H}_{36}\text{N}_9\text{O}_8\text{Tb}$ : C, 46.1; H, 4.35; N, 15.1 %:

Formula derived from crystallography:  $(\text{NH}_4)\text{Dy}(\mathbf{2-4H})(\text{H}_2\text{O})_{3.09}(\text{CH}_3\text{CN})$

Calculated for  $\text{C}_{34}\text{H}_{37}\text{DyN}_{10}\text{O}_7$ : C, 47.5; H, 4.34; N, 16.3 %:

Found: C, 47.5; H, 4.23, N 16.4 %

Formula derived from crystallography:  $(\text{NH}_4)\text{Ho}(\mathbf{2-4H})(\text{H}_2\text{O})_{3.10}(\text{CH}_3\text{CN})$

Calculated for  $\text{C}_{34}\text{H}_{37}\text{HoN}_{10}\text{O}_7$ : C, 47.3; H, 4.32; N, 16.2 %:

Found: C, 47.5; H, 4.30, N 16.3 %

Formula derived from crystallography:  $(\text{NH}_4)\text{Er}(\mathbf{2-4H})(\text{H}_2\text{O})_{3.11}(\text{CH}_3\text{CN})$

Calculated for  $\text{C}_{34}\text{H}_{37}\text{ErN}_{10}\text{O}_7$ : C, 47.2; H, 4.31; N, 16.2 %:

Found: C, 47.3; H, 4.28, N 16.2 %

Formula derived from crystallography:  $(\text{NH}_4)\text{Yb}(\mathbf{2-4H})(\text{H}_2\text{O})_{3.15}(\text{CH}_3\text{CN})$

Calculated for  $\text{C}_{34}\text{H}_{37}\text{N}_{10}\text{O}_7\text{Yb}$ : C, 46.9; H, 4.28; N, 16.1 %:

Found: C, 46.9; H, 4.35, N 16.0 %

Complexes of **3** crystallised from ethanol/ethyl acetate

Formula derived from crystallography:  $(\text{NH}_4)\text{Eu}(\mathbf{3-4H})(\text{EtOH})_4$

Calculated for  $\text{C}_{52}\text{H}_{68}\text{EuN}_9\text{O}_8$ : C, 56.8; H, 6.24; N, 11.5 %

Found: C, 53.7; H, 5.19, N 12.7 %

Revised formula:  $(\text{NH}_4)\text{Eu}(\mathbf{3-4H})(\text{H}_2\text{O})_4$

Calculated for  $\text{C}_{44}\text{H}_{52}\text{EuN}_9\text{O}_8$ : C, 53.6; H, 5.31; N, 12.8 %

Formula derived from crystallography:  $(\text{NH}_4)\text{Gd}(\mathbf{3-4H})(\text{EtOH})_4$

Calculated for  $\text{C}_{52}\text{H}_{68}\text{GdN}_9\text{O}_8$ : C, 56.6; H, 6.21; N, 11.4 %

Found: C, 52.7; H, 5.07, N 12.5 %

Revised formula:  $(\text{NH}_4)\text{Gd}(\mathbf{3-4H})(\text{H}_2\text{O})_5$

Calculated for  $\text{C}_{44}\text{H}_{52}\text{GdN}_9\text{O}_8$ : C, 52.3; H, 5.39; N, 12.5 %

### Crystal Structure Supplementary Information

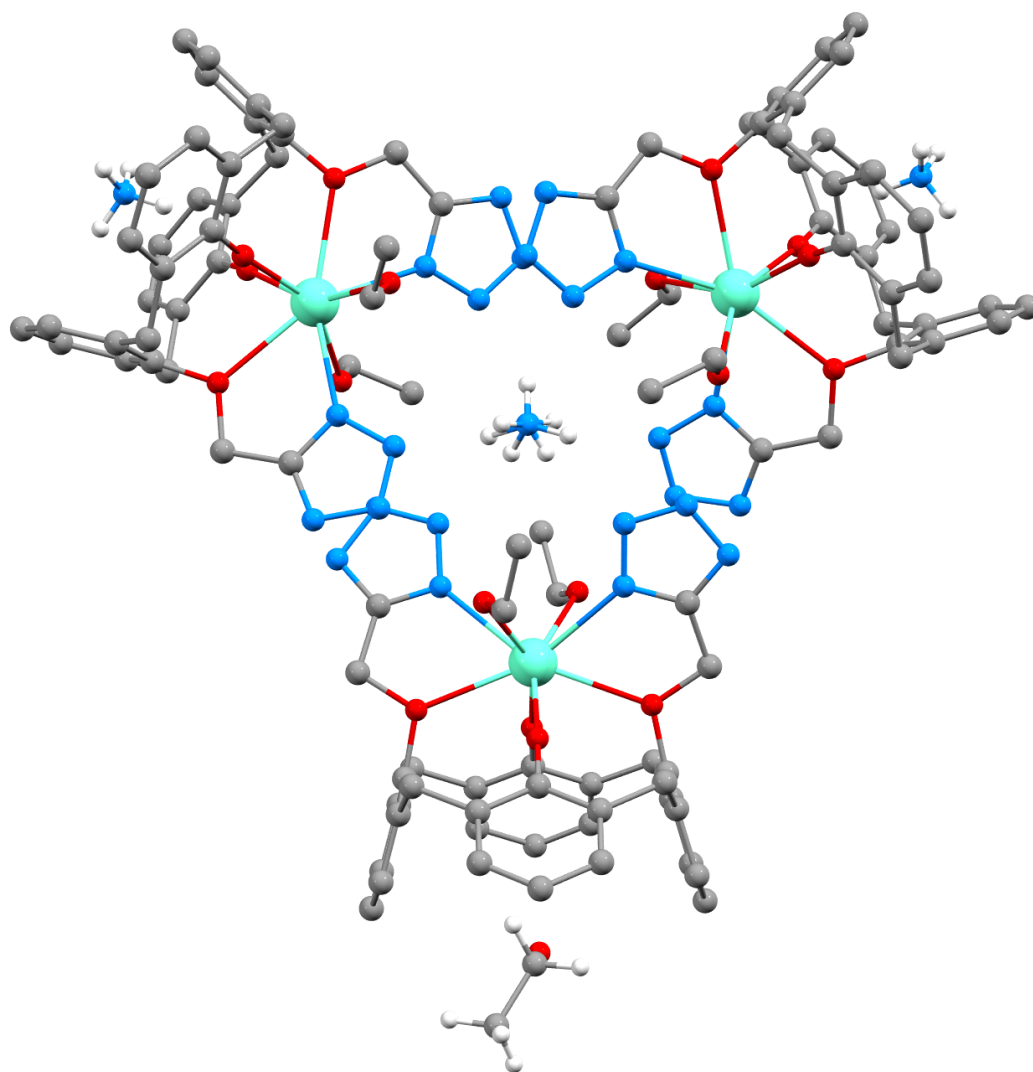


Figure S8. The trimeric structure positioned about the disordered N2 ammonium cation in  $(\text{NH}_4)[\text{Eu}(\mathbf{2-4H})(\text{HOEt})_2] \cdot 2\text{EtOH}$ .



Table S1 Hydrogen bonds for  $(\text{NH}_4)[\text{Eu}(\mathbf{2-4H})(\text{HOEt})_2] \cdot 2\text{EtOH}$  [ $\text{\AA}$  and  $^\circ$ ].

D-H...A	d(D-H)	d(H...A)	d(D...A)	$\angle(\text{DHA})$
O(101)-H(101)...N(314) <sup>1</sup>	0.84(2)	1.99(4)	2.806(8)	163(10)
O(201)-H(201)...N(514)	0.85(2)	1.88(3)	2.720(7)	166(6)
O(301)-H(301)...N(114)	0.83(2)	2.03(3)	2.833(7)	161(6)
O(401)-H(401)...N(515)	0.85(2)	2.02(5)	2.804(9)	155(8)
O(501)-H(501)...N(115)	0.86(2)	2.05(4)	2.845(9)	154(7)
N(1)-H(1AN)...O(401) <sup>2</sup>	0.895(17)	1.98(3)	2.831(9)	158(5)
N(1)-H(1DN)...O(21)	0.883(17)	2.32(3)	3.159(7)	159(5)
N(2)-H(2AN)...N(513)	0.880(18)	2.18(3)	2.907(16)	139(5)
N(2)-H(2BN)...N(313)	0.890(18)	2.379(19)	2.883(15)	116.0(10)
N(2)-H(2BN)...N(313) <sup>1</sup>	0.890(18)	2.379(19)	3.201(13)	153.5(14)

Symmetry transformations used to generate equivalent atoms:

<sup>1</sup>  $1-x, y, 1/2-z$ ; <sup>2</sup>  $1/2-x, y-1/2, 1/2-z$

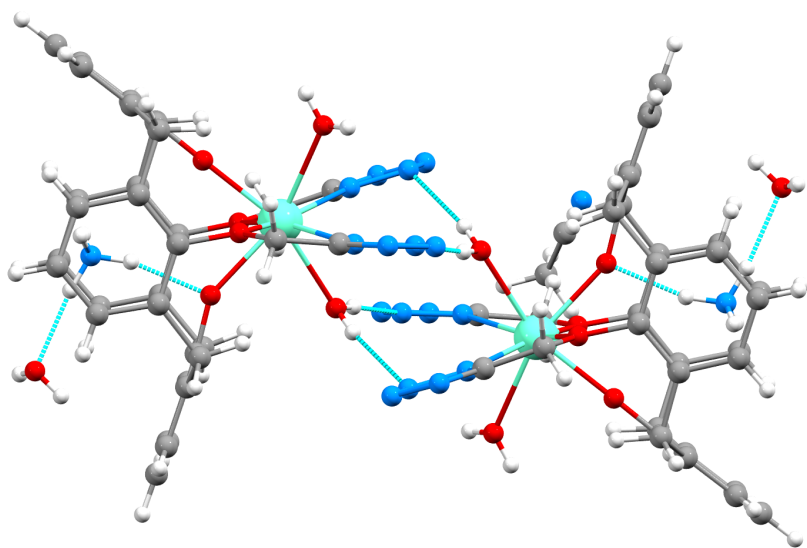


Figure S9. The dimeric structure in  $(\text{NH}_4)[\text{Eu}(\mathbf{2-4H})(\text{OH}_2)_2] \cdot \text{CH}_3\text{CN} \cdot \text{H}_2\text{O}$ , linked by hydrogen bonds between coordinated water molecules and tetrazole N atoms.

Table S2 Hydrogen bonds for  $(\text{NH}_4)[\text{Eu}(\mathbf{2-4H})(\text{OH}_2)_2]\cdot\text{CH}_3\text{CN}\cdot\text{H}_2\text{O}$  [ $\text{\AA}$  and  $^\circ$ ].

D-H...A	d(D-H)	d(H...A)	d(D...A)	$\angle(\text{DHA})$
O(1)-H(1AO)...N(315) <sup>1</sup>	0.824(16)	2.01(2)	2.7858(17)	157(3)
O(1)-H(1BO)...O(3) <sup>2</sup>	0.806(16)	2.35(2)	3.0535(19)	146(3)
O(2)-H(2AO)...N(113) <sup>3</sup>	0.807(15)	2.024(16)	2.8206(18)	169(2)
O(2)-H(2BO)...N(313) <sup>3</sup>	0.827(15)	1.942(16)	2.7624(18)	172(2)
O(3)-H(3AO)...N(115) <sup>4</sup>	0.831(17)	2.12(2)	2.919(2)	162(3)
N(1)-H(1AN)...O(41)	0.897(17)	1.916(18)	2.7922(18)	165(3)
N(1)-H(1BN)...O(3)	0.896(17)	1.948(17)	2.837(2)	171(3)

Symmetry transformations used to generate equivalent atoms:

<sup>1</sup> 2-x,1-y,1-z; <sup>2</sup> 3/2-x,1/2+y,1/2-z; <sup>3</sup> 1-x,1-y,1-z; <sup>4</sup> 1/2-x,-1/2+y,1/2-z

Table S3 Selected bond lengths [Å] for  $(\text{NH}_4)[\text{Ln}(\mathbf{2-4H})(\text{OH}_2)_2]\cdot\text{CH}_3\text{CN}\cdot 1.\text{XH}_2\text{O}$ .

---

	Eu	Gd	Dy	Ho	Er	Yb
Ln(1)-O(21)	2.1838(11)	2.1737(19)	2.1421(19)	2.1431(14)	2.1347(15)	2.1161(14)
Ln(1)-O(41)	2.2541(11)	2.2424(19)	2.2222(18)	2.2066(14)	2.1957(15)	2.1716(13)
Ln(1)-O(2)	2.4259(11)	2.4179(19)	2.3813(19)	2.3766(15)	2.3704(15)	2.3447(13)
Ln(1)-O(1)	2.4924(12)	2.480(2)	2.456(2)	2.4385(16)	2.4269(17)	2.4007(15)
Ln(1)-N(312)	2.5380(13)	2.521(2)	2.498(2)	2.4831(17))	2.4649(18)	2.4441(16)
Ln(1)-N(112)	2.5626(13)	2.547(2)	2.519(2)	2.4990(17))	2.4836(18)	2.4616(16)
Ln(1)-O(11)	2.6000(11)	2.5850(17)	2.5629(17)	2.5477(14)	2.5376(14)	2.5214(13)
Ln(1)-O(31)	2.6085(11)	2.5934(18)	2.5724(17)	2.5629(14)	2.5522(14)	2.5394(13)

---

Table S4 Hydrogen bonds for  $\{(NH_4)[Eu(3-4H)(HOEt)] \cdot 2EtOH \cdot H_2O\}_n$  [ $\text{\AA}$  and  $^\circ$ ].

D-H...A	d(D-H)	d(H...A)	d(D...A)	<(DHA)
O(201)-H(201)...N(313)	0.84	2.14	2.883(17)	147.0
O(301)-H(301)...N(114) <sup>1</sup>	0.84	2.03	2.764(17)	145.7
O(101)-H(101)...O(201) <sup>2</sup>	0.84(7)	1.89(10)	2.634(15)	147(16)
N(1)-H(1AN)...O(1)	0.83(6)	2.24(10)	2.873(19)	134(12)
N(1)-H(1BN)...O(301)	0.84(6)	1.89(5)	2.700(17)	161(13)
N(1)-H(1CN)...O(41)	0.84(6)	2.18(7)	2.963(15)	153(12)
O(1)-H(1BO)...N(115) <sup>1</sup>	0.82(11)	2.03(12)	2.849(18)	172(21)

Symmetry transformations used to generate equivalent atoms:

<sup>1</sup>  $x+1/2, 1/2-y, z+1/2$ ; <sup>2</sup>  $x, 1-y, z+1/2$

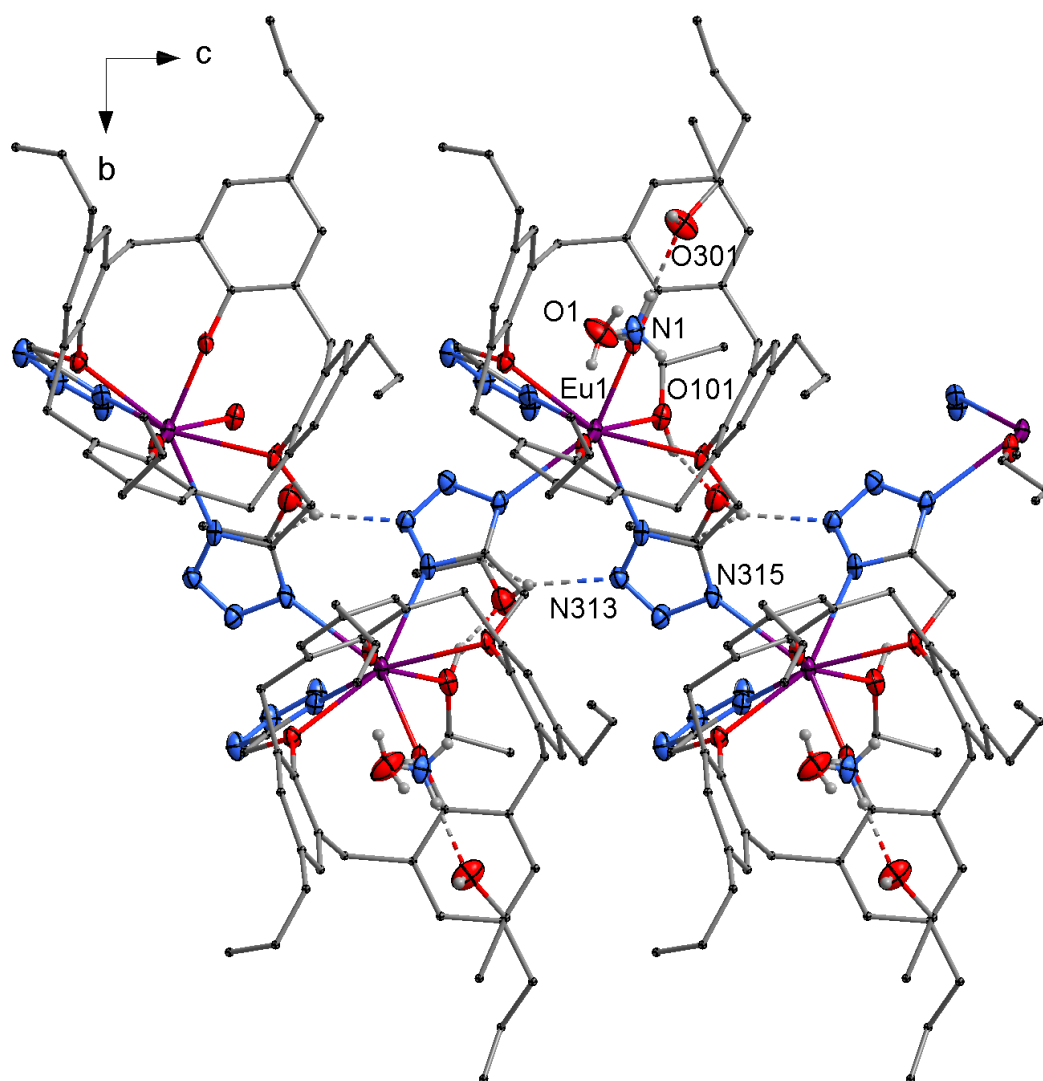


Figure S10. Structure of  $\{(\text{NH}_4)[\text{Eu}(\mathbf{3-4H})(\text{HOEt})]\cdot 2\text{EtOH}\cdot \text{H}_2\text{O}\}_n$  projected along the  $a$ -axis showing the hydrogen bonding within the polymer. Hydrogen atoms not involved in the hydrogen bonding have been omitted.

## Solution phase photophysical studies of Ln complexes of calixarene 2

Emission was observed in both the visible (europium, terbium, dysprosium), as well as near-infrared (ytterbium), regions of the electromagnetic spectrum when the deprotonated debutylated di-tetrazole calixarene **2** ligand was employed. The characteristic emission profiles associated with the lanthanoid element and each of their specific transitions are reported.

All of the experiments were conducted by adding two equivalents of the respective lanthanoid ions in the  $5 \times 10^{-5}$  M solution containing the ligand deprotonated with excess triethylamine base in acetonitrile, which was then excited at 300 nm at 298 K. All of the blank solutions with two equivalents of the respective free lanthanoid ions have negligible emissions when compared with the experimental values.

The following Figures shows the combined excitation and emission spectra of the ligand with the respective lanthanoid ions. From observing the excitation profile, there are some indications that the emission derived from the direct excitation of the lanthanoid ion.

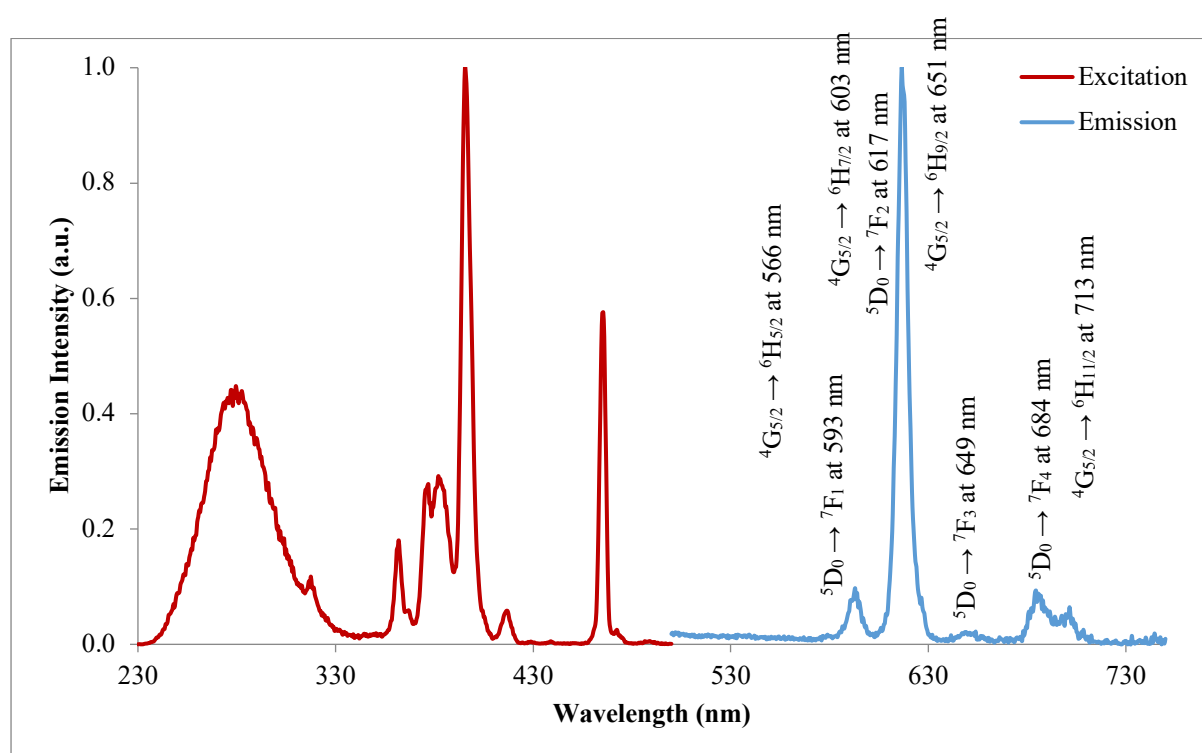


Figure S11. Normalised excitation and emission spectra of Eu-2 in acetonitrile.

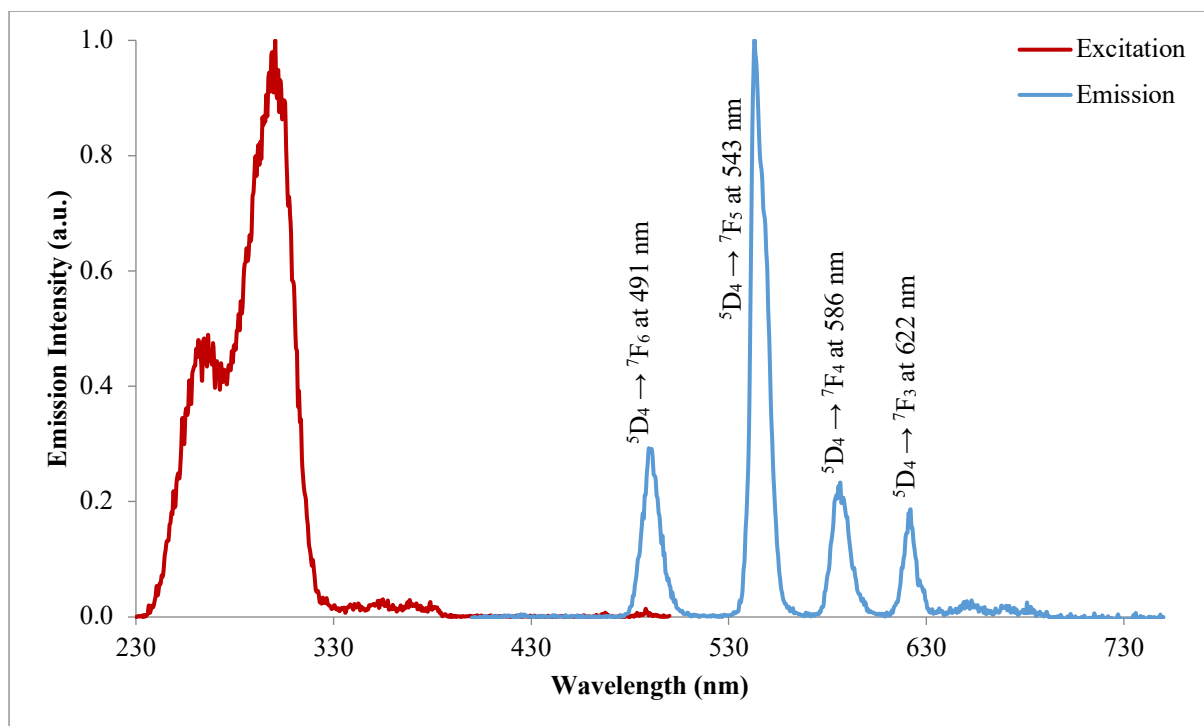


Figure S12. Normalised excitation and emission spectra of Tb-2 in acetonitrile.

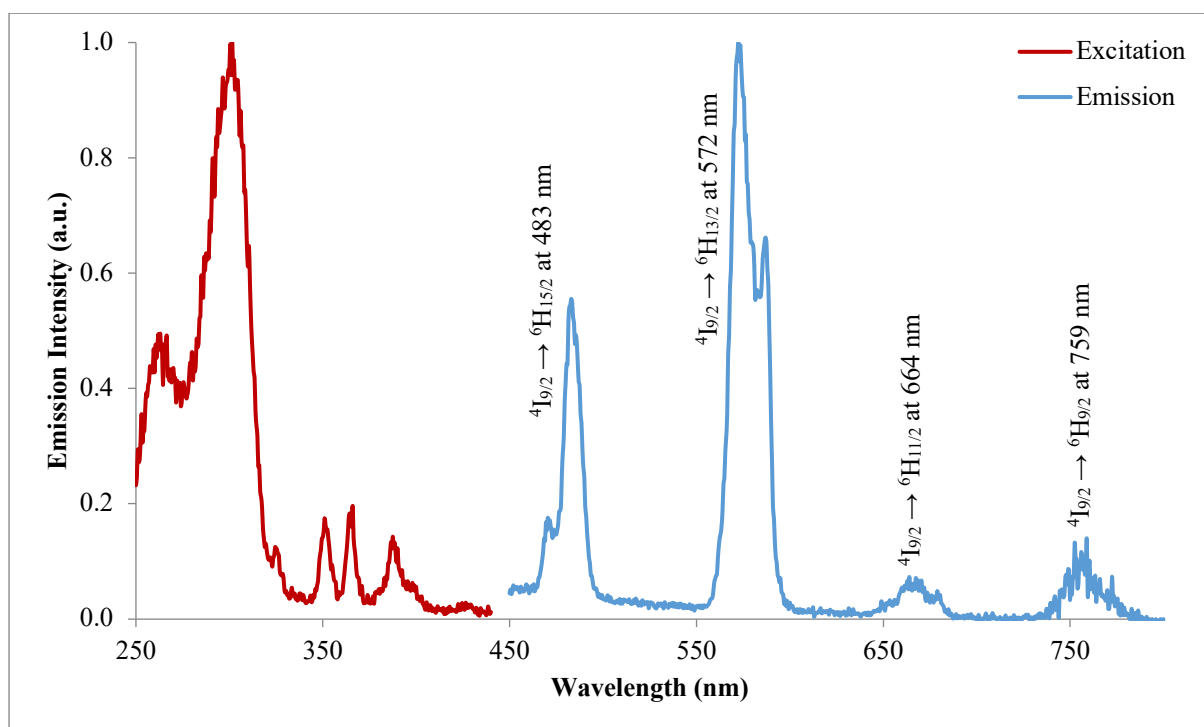


Figure S13. . Normalised excitation and emission spectra of Dy-2 in acetonitrile.

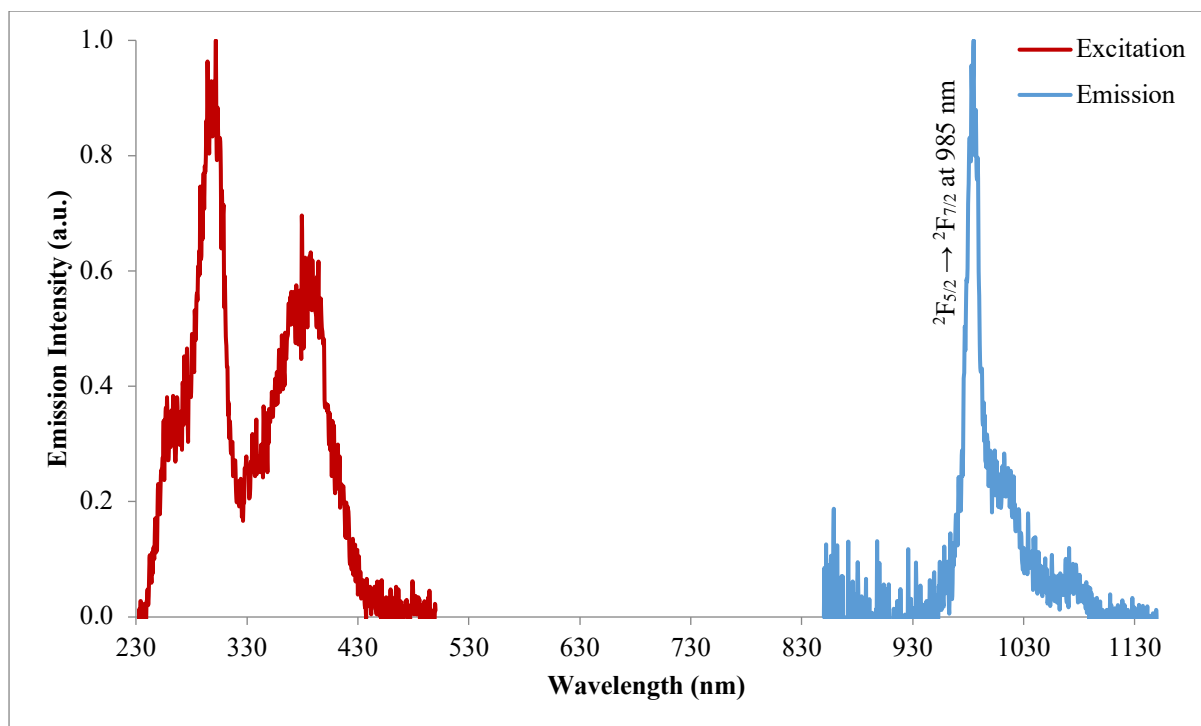


Figure S14. . Normalised excitation and emission spectra of Yb-2 in acetonitrile.

## References

- [1] Y. Liu, G. Huang, H. Y. Zhang, *J. Mol. Struct.* **2002**, *608*, 213-217.
- [2] Y. J. Chen, W. S. Chung, *Eur. J. Org. Chem.* **2009**, 4770-4776.
- [3] C. D. Gutsche, J. A. Levine, P. K. Sujeeth, *J. Org. Chem.* **1985**, *50*, 5802-5806.
- [4] L. Semenova, B. Skelton, A. White, *Aust. J. Chem.* **1996**, *49*, 997-1004.